

# Numerical Approximations of a Traffic Flow Model on Networks

GABRIELLA BRETTI, ROBERTO NATALINI, BENEDETTO PICCOLI \*

## Abstract

We consider a mathematical model for fluid-dynamic flows on networks which is based on conservation laws. Road networks are considered as graphs composed by arcs that meet at some junctions. The crucial point is represented by junctions, where interactions occur and the problem is underdetermined. The approximation of scalar conservation laws along arcs is carried out by using conservative methods, such as the classical Godunov scheme and the more recent discrete velocities kinetic schemes with the use of suitable boundary conditions at junctions. Riemann problems are solved by means of a simulation algorithm which proceeds processing each junction. We present the algorithm and its application to some simple test cases and to portions of urban network.

*Key Words:* scalar conservation laws, traffic flow, fluid-dynamic models, finite difference schemes, boundary conditions.

*AMS Subject Classifications:* Primary 65M06. Secondary 90B20, 35L65, 34B45, 90B10.

---

\*Istituto per le Applicazioni del Calcolo "M. Picone", Viale del Policlinico 137, 00161 - Roma, Italy; E-mail: [g.bretti@iac.cnr.it](mailto:g.bretti@iac.cnr.it), [r.natalini@iac.cnr.it](mailto:r.natalini@iac.cnr.it), [b.piccoli@iac.cnr.it](mailto:b.piccoli@iac.cnr.it)

# 1 Introduction.

The study of traffic flow aims to understand traffic behavior in urban context in order to answer to several questions: where to install traffic lights or stop signs; how long the cycle of traffic lights should be; where to construct entrances, exits, and overpasses. The aims of this analysis are principally represented by the maximization of cars flow, and the minimization of traffic congestions, accidents and pollution. In general, network models of transportation systems are assumed to be static, but these models do not allow a correct simulation of heavily congested urban road networks. For this reason, traffic engineers have started to consider some alternative models, often referred to as **DTA** (dynamic traffic assignment) or *within-day* models, see the review paper [2] and references therein. The use of within-day modeling makes necessary to give a new formulation of the problem: we have to solve the DNL (dynamic network loading) problem, that is, the reproduction of the traffic flow motion on the network, which requires the introduction of time advancing mathematical models (traffic simulation models). However, the main problems in DNL models are the fact that they do not properly reproduce the backward propagation of shocks and the difficulty of collecting experimental data to test the models.

Microscopic models, which form a widely used class of models, are characterized by the fact that they are sensitive to small perturbations. On the other hand, it can be difficult to give a qualitative description and visualization of phenomena on a macroscopic scale.

Here we deal with the fluid-dynamic models proposed in [7, 8], which can be seen as a macroscopic model with some traffic regulation strategies (within-day models) and which allows to observe the network in the time evolution through waves formation. In the 1950s James Lighthill and Gerald Whitham in [16], and independently Richards in [18], proposed to apply fluid dynamics concepts to traffic. In a single road, this nonlinear model is based on the conservation of cars described by the scalar hyperbolic conservation law:

$$\partial_t \rho + \partial_x f(\rho) = 0, \quad (1.1)$$

where  $\rho = \rho(t, x) \in [0, \rho_{max}]$  is the density of cars,  $(t, x) \in \mathbb{R}^2$  and  $\rho_{max} > 0$  is the maximum density of cars on the road. The function  $f(\rho)$  is the flux of cars, which is written as product of the density and of the local speed of cars  $v$ : i.e.  $f(\rho) = \rho v$ . In most cases, and at least as a first order approximation, one can assume that  $v$  is a decreasing function, only depending on the density, and that the corresponding flux is a concave function. We refer to [12, 19] for more details and comments on the single road models. Let us remark that fluid-dynamic models for traffic flow seem to be the most appropriate to detect macroscopic phenomena as shocks formation and propagation of waves backwards along roads. However, they can develop discontinuities in a finite time even starting from smooth initial data, then needing for a careful definition of the analytical framework, and an even greater consideration of suitable numerical schemes. We refer to [5, 9] for an updated account of the theory of general hyperbolic conservation laws, and to [11, 15] for a standard introduction to the

main numerical ideas. Notice that, in all this classical works on traffic flows, only a single road was taken into account. More recently, in [7, 8, 13, 14], some models have been proposed for traffic flow on road networks. Following [8], we focus on a road network composed by a finite number of roads parametrized by intervals  $[a_i, b_i]$  that meet at some junctions. Junctions play a key role, as the system at a junction is underdetermined even after prescribing the conservation of cars, that can be written as the Rankine-Hugoniot condition:

$$\sum_{i=1}^n f(\rho_i(t, b_i)) = \sum_{j=n+1}^{n+m} f(\rho_j(t, a_j)),$$

where  $\rho_i$ ,  $i = 1, \dots, n$ , are the car densities on incoming roads;  $\rho_j$ ,  $j = n + 1, \dots, n + m$ , are the car densities on outgoing roads. Such relation expresses the equality of ingoing and outgoing fluxes. For endpoints that do not touch a junction (and are not infinite), we assume to have a given boundary data and solve the corresponding boundary problem, as in [4]. Let us remark that, in this paper, traffic lights will not be considered, since their analytical and numerical theory is already well understood [19].

As in [8], we make the following two assumptions: there are some distribution coefficients of traffic from incoming roads to outgoing roads; drivers behave in such a way to maximize fluxes whenever is possible. One could also treat junctions where the number of incoming roads is greater than the number of outgoing ones, not covered by the analysis of [8]. In particular, we are interested in the case of two incoming and one outgoing roads. In this case, the two distribution coefficients of the incoming roads must be equal to one, thus determining a loss of uniqueness for the solutions. This is not a purely mathematical issue, but it is rather due to the fact that if not all cars can go through the junction then there should be a yielding rule between incoming roads. To treat this case we introduce a new parameter  $q \in ]0, 1[$ , the *right of way* (see [7]), which permits to uniquely solve Riemann problems. In particular, it indicates which, among cars passing through the junction, is the percentage of cars coming from the first incoming road and which is the percentage coming from the second road. The details about the mentioned rules are discussed in Section 2.

We deal with the numerical approximation of the possibly discontinuous solutions produced by this model. In particular, the main contribution of the paper is represented by the introduction of suitable boundary conditions at the junctions for classical and less classical numerical schemes. These schemes, namely Godunov scheme and Kinetic methods, adapted to the problem, provide approximations which are quite stable as we will show later through many numerical tests.

The paper is organized as follows. Section 2 is devoted to the description of the model. Some examples of simple networks are proposed in Section 3. In Section 4 we describe the numerical schemes with the particular boundary conditions used to produce approximated solutions of the problem. In Section 5 we give an extended presentation of some numerical experiments which show the effectiveness of our approximation.

## 2 Backgrounds

We consider the conservation of cars described by the equation [16, 18]:

$$\partial_t \rho + \partial_x f(\rho) = 0, \quad (2.1)$$

where  $\rho = \rho(t, x)$  is the density of cars, with  $\rho \in [0, \rho_{max}]$ ,  $(t, x) \in \mathbb{R}^2$  and  $\rho_{max}$  is the maximum density of cars on the road;  $f(\rho)$  is the flux, which can be written  $f(\rho) = \rho v(\rho)$ , with  $v(t, x)$  the velocity. Typically  $v$  is a smooth decreasing function of  $\rho$ .

For equation (2.1) on  $\mathbb{R}$  it is well-known that there exists a unique weak entropy solution for every initial data belonging to  $L^\infty$ , with a continuous dependence on the initial data in  $L^1_{loc}$ .

Here we are interested in a road network, which is a finite number of roads modeled by intervals  $[a_i, b_i]$  (with one of the endpoints eventually infinite) that meet at some junctions. We give boundary data and solve the associated boundary problem for the endpoints (not infinite) that do not meet at any junction. Junctions play a fundamental role, since the system at a junction is underdetermined even imposing the conservation of cars, expressed by the Rankine-Hugoniot condition:

$$\sum_{i=1}^n f(\rho_i(t, b_i)) = \sum_{j=n+1}^{n+m} f(\rho_j(t, a_j)),$$

where  $\rho_i$ ,  $i = 1, \dots, n$ , are the car densities on incoming roads;  $\rho_j$ ,  $j = n + 1, \dots, n + m$ , are the car densities on the outgoing roads.

To determine a unique solution to Riemann problems at junctions, assume the following criteria:

- (A) there are some fixed coefficients, the prescribed preferences of drivers, that express the distribution of traffic from incoming to outgoing roads;
- (B) respecting (A), drivers choices are made in order to maximize the flux.

Let us consider the rule (A). We fix a matrix, called **traffic distribution matrix**:

$$A = \{\alpha_{ji}\}_{j=n+1, \dots, n+m, i=1, \dots, n} \in \mathbb{R}^{m \times n},$$

such that

$$0 < \alpha_{ji} < 1, \quad \sum_{j=n+1}^{n+m} \alpha_{ji} = 1, \quad (2.2)$$

for  $i = 1, \dots, n$  and  $j = n + 1, \dots, n + m$ , where  $\alpha_{ji}$  is the percentage of drivers arriving from the  $i$ -th incoming road that take the  $j$ -th outgoing road.

**Remark 2.1** *Note that the only the rule (A) is not sufficient to have a unique solution to Riemann problems, that are still under-determined.*

Under suitable assumptions on  $A$  and rules (A)-(B), representing a situation where drivers have a final destination and maximize the flux whenever is possible, Riemann problems can be uniquely solved. In [8] it was proved existence of each solution to Cauchy problems respecting rules (A) and (B).

Let us fix  $m < n$ . In this case it is necessary to introduce a further rule, see [7]. In particular, consider the case  $m = 1, n = 2$ . The two coefficients  $\alpha_{31}$  and  $\alpha_{32}$  must be equal to one. This is due to the fact that if not all cars can go through the junction, then there should be a yielding rule between incoming roads. Therefore we fix a new *right of way* parameter  $q \in ]0, 1[$  and assign the rule:

- (C) Assume that not all cars can enter the outgoing road and let  $C$  be the quantity that can do it. Then  $qC$  cars come from first incoming road and  $(1 - q)C$  cars from the second.

The rule (C) allows us to uniquely solve Riemann problems.

It is possible to introduce time dependent coefficients for the rule (A) and we can treat networks assigning a different flux function  $f_i$  on each road  $I_i$ .

Let us first recall the basic definitions and results from [8]. The parametrization of roads composing a network is made through a set of intervals  $I_i = [a_i, b_i] \subset \mathbb{R}$ ,  $i \in 1, \dots, N$ , with the endpoints possibly infinite. The datum is a finite collection of densities  $\rho_i$  defined on  $I_i \times [0, +\infty)$ . Roads are linked to each other by some junctions and each road can be incoming at most for one junction and outgoing at most for one junction. Consequently the complete model is given by a pair  $(\mathcal{I}, \mathcal{J})$ , with  $\mathcal{I} = \{I_i : i = 1, \dots, N\}$  the collection of roads and  $\mathcal{J}$  the number of junctions.

Consider a junction  $J$  with  $n$  incoming roads, say  $I_1, \dots, I_n$ , and  $m$  outgoing roads, say  $I_{n+1}, \dots, I_{n+m}$ . A *weak solution at the junction  $J$*  is a collection of functions  $\rho_l : [0, +\infty[ \times I_l \rightarrow \mathbb{R}$ ,  $l = 1, \dots, n + m$ , such that

$$\sum_{l=0}^{n+m} \left( \int_0^{+\infty} \int_{a_l}^{b_l} \left( \rho_l \frac{\partial \varphi_l}{\partial t} + f(\rho_l) \frac{\partial \varphi_l}{\partial x} \right) dx dt \right) = 0, \quad (2.3)$$

for every  $\varphi_l$ ,  $l = 1, \dots, n + m$ , smooth having compact support in  $(0, +\infty) \times (a_l, b_l]$  for  $l = 1, \dots, n$  (incoming roads) and in  $(0, +\infty) \times [a_l, b_l)$  for  $l = n + 1, \dots, n + m$  (outgoing roads), that are also smooth across the junction.

**Remark 2.2** Let  $\rho = (\rho_1, \dots, \rho_{n+m})$  be a weak solution at the junction such that each  $x \rightarrow \rho_i(t, x)$  has bounded variation. We can deduce that  $\rho$  satisfies the Rankine-Hugoniot Condition at the junction  $J$ , for almost every  $t > 0$ .

The rules (A) and (B) can be explicitly given only for solutions with bounded variation as defined in [8]. Boundary data are assigned at the endpoints not infinite that do not touch any junction and they are imposed in the sense of [4]. We recall the construction of solutions to the Riemann problems for rules (A) and (B). For a junction, as for a scalar conservation law, a Riemann problem is a Cauchy problem with an initial data of Heaviside type on each road. Once

Riemann problems are solved, a solution to Cauchy problems can be obtained, for instance, by wave front tracking. In case of concave or convex fluxes, the Riemann solutions are of two types: continuous waves called rarefactions and travelling discontinuities called shocks.

Let us make the following assumption on the flux:

( $\mathcal{F}$ )  $f : [0, 1] \rightarrow \mathbb{R}$  is smooth, strictly concave (i.e.  $f'' \leq -c < 0$  for some  $c > 0$ ),  $f(0) = f(1) = 0$ ,  $|f'(x)| \leq C < +\infty$ . Hence there exists a unique  $\sigma \in ]0, 1[$  such that  $f'(\sigma) = 0$  (that is  $\sigma$  is a strict maximum).

The densities of cars on the incoming roads are indicated by  $\rho_i(t, x) : \mathbb{R}^+ \times I_i \rightarrow [0, 1]$ ,  $i \in \{1, \dots, n\}$  and on the outgoing roads  $\rho_j(t, x) : \mathbb{R}^+ \times I_j \rightarrow [0, 1]$ ,  $j \in \{1, \dots, m\}$ . We introduce the following application:

**Definition 2.1** Let  $\tau : [0, 1] \mapsto [0, 1]$ ,  $\tau(\sigma) = \sigma$ , be the well-defined map satisfying the following

$$\tau(\rho) \neq \rho, \quad f(\tau(\rho)) = f(\rho),$$

for each  $\rho \neq \sigma$ .

Uniqueness of the solution to Riemann problems can be ensured under some generic additional conditions on the matrix  $A$ . Let  $\{e_1, \dots, e_n\}$  be the canonical basis of  $\mathbb{R}^n$  and for every subset  $V \subset \mathbb{R}^n$ , with  $V^\perp$  its orthogonal. For every  $i = 1, \dots, n$  define  $H_i$  the coordinate hyperplane orthogonal to  $e_i$  and for every  $j = n+1, \dots, n+m$  define  $H_j = \alpha_j^\perp$ , with  $\alpha_j = (\alpha_{j1}, \dots, \alpha_{jn})$ . If  $\mathcal{K}$  is the set of indices  $k = (k_1, \dots, k_l)$ ,  $1 \leq l \leq n-1$ , such that  $0 \leq k_1 < k_2 < \dots < k_l \leq n+m$  and for every  $k \in \mathcal{K}$  we set

$$H_k = \bigcap_{h=1}^l H_{k_h}.$$

Letting  $\mathbf{1} = (1, \dots, 1) \in \mathbb{R}^n$ , we assume

( $RP$ ) for every  $k \in \mathcal{K}$ ,  $\mathbf{1} \notin \mathbf{H}_k^\perp$ .

From ( $RP$ ) easily follows  $m \geq n$ , for details see [8].

The existence and uniqueness of admissible solutions for the Riemann problem of a junction is expressed by the next Theorem.

**Theorem 2.3** Let  $f : [0, 1] \rightarrow \mathbb{R}$  satisfy ( $\mathcal{F}$ ), the matrix  $A$  satisfy ( $C$ ) and  $\rho_{1,0}, \dots, \rho_{n+m,0} \in [0, 1]$  be constants. There exists a unique admissible (with bounded variation) weak solution.

For the proof see [8].

Let us show the procedure to construct solutions. Define the map

$$E : (\gamma_1, \dots, \gamma_n) \in \mathbb{R}^n \mapsto \sum_{i=1}^n \gamma_i$$

and the sets

$$\Omega_i \doteq [0, f(\bar{\rho}_{i,0})] \quad i = 1, \dots, n, \quad \Omega_j \doteq [0, f(\bar{\rho}_{j,0})] \quad j = n+1, \dots, n+m,$$

where

$$\bar{\rho}_{i,0} = \begin{cases} \rho_{i,0}, & \text{if } 0 \leq \rho_{i,0} \leq \sigma, \\ \sigma, & \text{if } \sigma \leq \rho_{i,0} \leq 1, \end{cases} \quad i = 1, \dots, n,$$

$$\bar{\rho}_{j,0} = \begin{cases} \sigma, & \text{if } 0 \leq \rho_{j,0} \leq \sigma, \\ \rho_{j,0}, & \text{if } \sigma \leq \rho_{j,0} \leq 1, \end{cases} \quad j = n+1, \dots, n+m,$$

$$\Omega \doteq \left\{ (\gamma_1, \dots, \gamma_n) \in \Omega_1 \times \dots \times \Omega_n \mid A \cdot (\gamma_1, \dots, \gamma_n)^T \in \Omega_{n+1} \times \dots \times \Omega_{n+m} \right\}.$$

The set  $\Omega$  is closed, convex and not empty. Moreover, by (RP) there exists a unique vector  $(\hat{\gamma}_1, \dots, \hat{\gamma}_n) \in \Omega$  such that

$$E(\hat{\gamma}_1, \dots, \hat{\gamma}_n) = \max_{(\gamma_1, \dots, \gamma_n) \in \Omega} E(\gamma_1, \dots, \gamma_n).$$

Once we have the maximum incoming fluxes  $\hat{\gamma}_i$  for  $i \in \{1, \dots, n\}$  thus satisfying rule (B), we choose  $\hat{\rho}_i \in [0, 1]$  such that

$$f(\hat{\rho}_i) = \hat{\gamma}_i, \quad \hat{\rho}_i \in \begin{cases} \{\rho_{i,0}\} \cup [\tau(\rho_{i,0}), 1], & \text{if } 0 \leq \rho_{i,0} \leq \sigma, \\ [\sigma, 1], & \text{if } \sigma \leq \rho_{i,0} \leq 1. \end{cases} \quad (2.4)$$

By  $(\mathcal{F})$ ,  $\hat{\rho}_i$  exists and is unique. Recalling rule (A) one derives

$$\hat{\gamma}_j \doteq \sum_{i=1}^n \alpha_{ji} \hat{\gamma}_i, \quad j = n+1, \dots, n+m,$$

then  $\hat{\rho}_j \in [0, 1]$  are such that

$$f(\hat{\rho}_j) = \hat{\gamma}_j, \quad \hat{\rho}_j \in \begin{cases} [0, \sigma], & \text{if } 0 \leq \rho_{j,0} \leq \sigma, \\ \{\rho_{j,0}\} \cup [0, \tau(\rho_{j,0})], & \text{if } \sigma \leq \rho_{j,0} \leq 1. \end{cases} \quad (2.5)$$

Since  $(\hat{\gamma}_1, \dots, \hat{\gamma}_n) \in \Omega$ ,  $\hat{\rho}_j$  exists and is unique for every  $j \in \{n+1, \dots, n+m\}$ . The solution on each road is given by the solution to Riemann problem with data  $(\rho_{i,0}, \hat{\rho}_i)$  for incoming roads and  $(\hat{\rho}_j, \rho_{j,0})$  for outgoing roads. The solution can be a shock:

$$\rho_i(t, x) = \begin{cases} \rho_{i,0} & \text{if } x \leq \frac{f(\hat{\rho}_i) - f(\rho_{i,0})}{\hat{\rho}_i - \rho_{i,0}} t, \\ \hat{\rho}_i & \text{otherwise,} \end{cases} \quad (2.6)$$

or a rarefaction:

$$\rho_i(t, x) = \begin{cases} \rho_{i,0} & \text{if } x \leq f'(\rho_{i,0})t, \\ (f')^{-1}\left(\frac{x}{t}\right) & \text{if } f'(\rho_{i,0})t \leq x \leq f'(\hat{\rho}_i)t, \\ \hat{\rho}_i & \text{if } x > f'(\hat{\rho}_i)t. \end{cases} \quad (2.7)$$

We have the following existence result: using solutions to Riemann problems and the fact that the speed of propagation is finite, one can use a wave front tracking algorithm to build a sequence of solutions to Cauchy problems as showed in [8]. In order to have admissible solutions to Riemann problems, we need to solve  $(\rho_{i,0}, \hat{\rho}_i)$  by waves with negative speed, while  $(\hat{\rho}_j, \rho_{j,0})$  is solved by waves with positive speed. This is equivalent to conditions (2.4) and (2.5).

### 3 Examples

#### 3.1 Bottleneck

The simplest application of the fluid-dynamic model presented in the previous Section is represented by the bottleneck, which is a layout of the road characterized by a narrow passage that can constitute a point of congestion.

We consider two different flux functions along the road, where the conservation of cars is always expressed by (2.1) endowed with initial and boundary conditions. In the largest part of the street the flux assumed is the following

$$f_1(\rho) = \rho(1 - \rho), \quad \rho \in [0, 1], \quad (3.1)$$

while, in the narrowest part of the street, the flux considered is

$$f_2(\rho) = \rho \left( 1 - \frac{3}{2}\rho \right), \quad \rho \in [0, 2/3]. \quad (3.2)$$

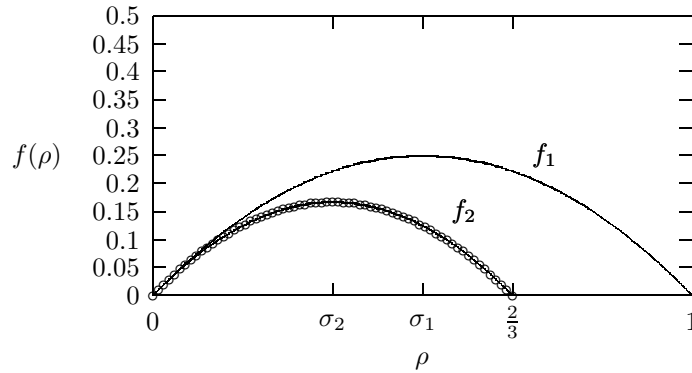


Figure 1: The flux functions  $f_1(\rho)$  and  $f_2(\rho)$ .

The maximum for the fluxes is unique:

$$f_1(\sigma_1) = \max_{[0,1]} f_1(\rho) = \frac{1}{4}, \quad \text{with } \sigma_1 = \frac{1}{2}, \quad (3.3)$$

$$f_2(\sigma_2) = \max_{[0,2/3]} f_2(\rho) = \frac{1}{6}, \quad \text{with } \sigma_2 = \frac{1}{3}. \quad (3.4)$$

A key role is played by the separation point between the two parts of the road, say  $S$ . Indicate by  $\rho_s$  the point placed on the left respect to  $S$  (that belongs to the widest part of the street) and by  $\rho_d$  the point of the narrowest part on the right respect to  $S$  so that we can consider the bottleneck as composed by



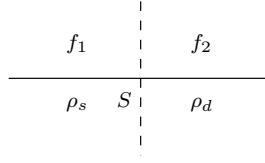


Figure 2: Interface at the bottleneck.

two roads. The maximization of  $f_1$  and  $f_2$  is performed following the rules, respectively

$$f_1^{max}(\rho) = \begin{cases} f_1(\rho_s) & \text{if } \rho_s \leq \sigma_1, \\ f_1(\sigma_1) & \text{if } \rho_s \geq \sigma_1, \end{cases}$$

$$f_2^{max}(u) = \begin{cases} f_2(\sigma_2) & \text{if } \rho_d \leq \sigma_2, \\ f_2(\rho_d) & \text{if } \rho_d \geq \sigma_2 \end{cases}$$

and the intersection point between the two intervals is obtained taking the minimum

$$\gamma = \min\{f_1^{max}(\rho_s), f_2^{max}(\rho_d)\}, \quad (3.5)$$

with  $\rho_s$  and  $\rho_d$  instantaneously fixed. As the maximum density allowed in the second part is given by  $\sigma_2 = \frac{1}{6}$ , the creation of queues occurs when the density on the first road verifies

$$\rho(1 - \rho) = \frac{1}{6} \iff \bar{\rho} = \frac{1 - \sqrt{\frac{1}{3}}}{2} \simeq 0.21. \quad (3.6)$$

Then, when  $\rho_{1,b} < \bar{\rho}$  (recall that  $\rho_{1,b}$  is the car density entering the largest road) there is no formation of shocks propagating backwards.

### 3.2 Two incoming and two outgoing roads

Here we consider the particular case of a junction with two outgoing and two incoming roads. The incoming roads are indicated as 1 e 2, while the outgoing roads are 3 and 4. In order to determine the region for the maximization of the

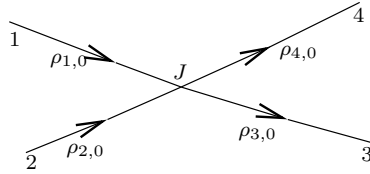


Figure 3: A junction with two incoming and two outgoing roads.

flux, we impose a restriction on the initial data. For roads  $i = 1, 2$  the maximum

flux reads:

$$f_i^{max} = \begin{cases} f(\sigma) & \text{if } \rho_{i,0} \in [\sigma, \rho_{max}] \\ f(\rho_{i,0}) & \text{if } \rho_{i,0} \in [0, \sigma), \end{cases}$$

while for roads  $j = 3, 4$  the maximum flux is:

$$f_j^{max} = \begin{cases} f(\sigma) & \text{if } \rho_{j,0} \in [0, \sigma] \\ f(\rho_{j,0}) & \text{if } \rho_{j,0} \in (\sigma, \rho_{max}]. \end{cases}$$

We obtain the two sets:

$$\Omega_{12} = [0, f(\bar{\rho}_{10})] \times [0, f(\bar{\rho}_{20})] \text{ and } \Omega_{34} = [0, f(\bar{\rho}_{30})] \times [0, f(\bar{\rho}_{40})]$$

and maximize the sum of fluxes on the region  $\Omega_{12} \cap A^{-1}(\Omega_{34})$ .

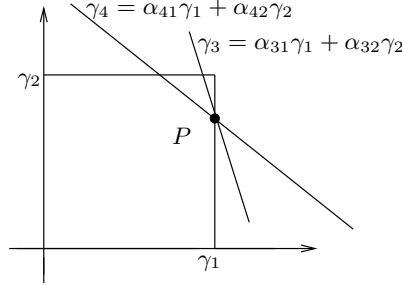


Figure 4: Maximization region.

Introducing the notation  $\gamma_l = f(\bar{\rho}_{l,0})$ ,  $l = 1, 2, 3, 4$ , we have

$$\max(\gamma_1 + \gamma_2) = \hat{\gamma}_1 + \hat{\gamma}_2$$

and we obtain  $\hat{\gamma}_3$  and  $\hat{\gamma}_4$ , through the following relation

$$A\hat{\gamma} \in \Omega_{34}, \quad (3.7)$$

where the traffic distribution matrix reads

$$A = \begin{pmatrix} \alpha_{31} & \alpha_{32} \\ \alpha_{41} & \alpha_{42} \end{pmatrix}. \quad (3.8)$$

The solution is:

$$(\hat{\gamma}_1, \hat{\gamma}_2, \hat{\gamma}_3, \hat{\gamma}_4)$$

and the corresponding  $\hat{\rho}_l$  are given by

$$f(\hat{\rho}_l) = \hat{\gamma}_l, \quad l = 1, \dots, 4. \quad (3.9)$$

In particular, we invert (3.9) using the following rules:

$$i = 1, 2, \quad \hat{\rho}_i \in \begin{cases} \{\rho_{i,0}\} \cup ]\tau(\rho_{i,0}), 1], & \text{if } 0 \leq \rho_{i,0} \leq \sigma, \\ [\sigma, 1], & \text{if } \sigma \leq \rho_{i,0} \leq 1, \end{cases} \quad (3.10)$$

$$j = 3, 4, \quad \hat{\rho}_j \in \begin{cases} [0, \sigma], & \text{if } 0 \leq \rho_{j,0} \leq \sigma, \\ \{\rho_{j,0}\} \cup [0, \tau(\rho_{j,0})[, & \text{if } \sigma \leq \rho_{j,0} \leq 1. \end{cases} \quad (3.11)$$

### 3.3 Two incoming and one outgoing roads

In order to show how rule (C) previously introduced works, let us consider a junction with one outgoing and two incoming roads. As explained in Section

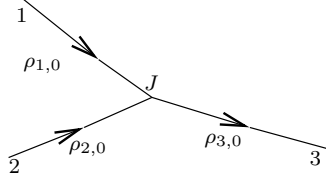


Figure 5: A junction with two incoming and one outgoing roads.

2, condition (RP) on  $A$  cannot hold for crossings with two incoming and one outgoing roads. Then we introduce a further parameter, namely  $q$ , with the following meaning: when the number of cars is too big to let all of them go through crossing, there is a yielding rule that describes the percentage of cars going through the crossing, that comes from the first road. Let us fix a crossing with two incoming roads  $[a_i, b_i]$ ,  $i = 1, 2$ , and one outgoing road  $[a_3, b_3]$  and assume that a right of way parameter  $q \in ]0, 1[$  is given. The solution to the Riemann problem  $(\rho_{1,0}, \rho_{2,0}, \rho_{3,0})$  is composed by a single wave on each road connecting the initial states to  $(\hat{\rho}_1, \hat{\rho}_2, \hat{\rho}_3)$  determined as follows (cfr. with the solution to the Riemann problem in the two incoming-two outgoing roads). Define  $\gamma_i^{max}$ ,  $i = 1, 2$  and  $\gamma_3^{max}$  in the following way:

$$\gamma_i^{max} = \begin{cases} f(\rho_{i,0}) & \text{if } \rho_{i,0} \in [0, \sigma], \\ f(\sigma) & \text{if } \rho_{i,0} \in ]\sigma, 1], \end{cases}$$

and

$$\gamma_3^{max} = \begin{cases} f(\sigma) & \text{if } \rho_{3,0} \in [0, \sigma], \\ f(\rho_{3,0}) & \text{if } \rho_{3,0} \in ]\sigma, 1]. \end{cases}$$

The quantities  $\gamma_i^{max}$  represent the maximum flux that can be reached by a single wave solution on each road. Since our goal is to maximize going through traffic, we set:

$$\hat{\gamma}_3 = \min\{\gamma_1^{max} + \gamma_2^{max}, \gamma_3^{max}\}. \quad (3.12)$$

Consider the space  $(\gamma_1, \gamma_2)$ , then rule (C) is respected by points on the line:

$$\gamma_2 = \frac{1-q}{q} \gamma_1. \quad (3.13)$$

Thus define  $P$  to be the point of intersection of the line (3.13) with the line  $\gamma_1 + \gamma_2 = \hat{\gamma}_3$ . Recall that the final fluxes should belong to the region:

$$\Omega = \{(\gamma_1, \gamma_2) : 0 \leq \gamma_i \leq \gamma_i^{max}\},$$

then we distinguish three cases:

- a)  $P$  is inside  $\Omega$ ,
- b)  $P$  is outside  $\Omega$ ,
- c)  $P$  is the upper-right vertex of  $\Omega$  (that corresponds to the case  $\hat{\gamma}_3 = \gamma_1^{max} + \gamma_2^{max}$ ).

In the first case we set  $(\hat{\gamma}_1, \hat{\gamma}_2) = P$ , while in the second we set  $(\hat{\gamma}_1, \hat{\gamma}_2) = Q$ , where  $Q$  is the point of the segment  $\Omega \cap \{(\gamma_1, \gamma_2) : \gamma_1 + \gamma_2 = \hat{\gamma}_3\}$  closest to the line (3.13). We show in Figure 6 the cases a)-b). In the third case, there is

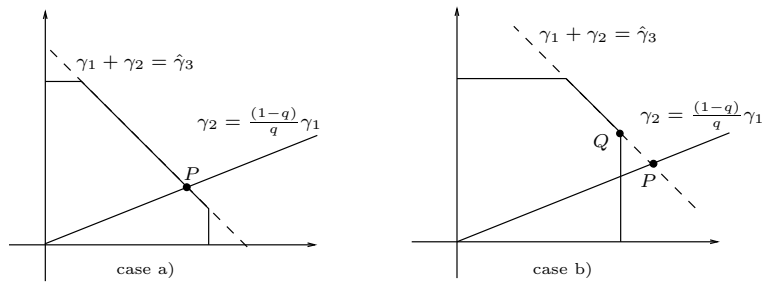


Figure 6: Solutions to Riemann problem for rule (C).

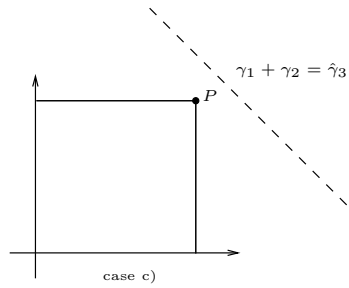


Figure 7: Solutions to Riemann problem without using rule (C).

no need of using rule (C) and  $(\hat{\gamma}_1, \hat{\gamma}_2) = P$ , see Figure 7. Then we determine  $\hat{\rho}_i$  with rules (2.4) and (2.5) presented in the previous Section.

### 3.4 Traffic circles

We consider the fluid dynamic model proposed in [8] adapted in a suitable way in order to treat the case of traffic circles. In fact, as explained in [7], a circle can be modeled using rule (C). Consider a general network, as the traffic circle, with junctions having either one incoming and two outgoing or two incoming and one outgoing roads. Therefore at each junction we can refer to the cases represented in paragraphs 3.2, 3.3. Once the solution to Riemann problems is fixed then we can introduce the definition of admissible solutions as in [7]. Similarly we can deal with the case of coefficients  $\alpha_{ij}$  and right of way parameters  $q_k$  depending on time.

Notice that we only treat the case of the single-lane traffic circles. A model for the multi-lane traffic circles is proposed in [7].

Consider a simple network representing a traffic circle composed by four roads, named  $1, \dots, 4$ , the first two incoming in the circle and the other two outgoing. In addition there are four roads  $1R, \dots, 4R$  that form the circle as in Figure 8. As before the parametrization of roads is given by  $[a_i, b_i]$ ,  $i = 1, \dots, 4$ , and

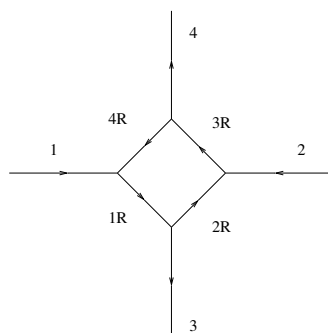


Figure 8: Traffic circle.

$[a_{iR}, b_{iR}]$ ,  $i = 1, \dots, 4$ . We assign a traffic distribution matrix  $A$  describing how traffic coming from roads 1, 2 distributes through roads 3 and 4, passing by the intermediate roads of the circle. Two parameters are fixed, namely  $\alpha, \beta \in ]0, 1[$ , such that

- (C1) If  $M$  cars reach the circle from road 1, then  $\alpha M$  drive to road 3 and  $(1 - \alpha)M$  drive to road 4,
- (C2) If  $M$  cars reach the circle from road 2, then  $\beta M$  drive to road 4 and  $(1 - \beta)M$  drive to road 3.

Then we can determine the distribution coefficients, see [7].

## 4 Numerical approximation

For definitiveness, we choose the following flux

$$f(\rho) = v_{max} \rho \left(1 - \frac{\rho}{\rho_{max}}\right), \quad (4.1)$$

and, setting for simplicity  $\rho_{max} = 1 = v_{max}$ :

$$f(\rho) = \rho(1 - \rho).$$

**Remark 4.1** *However, any concave flux could be assumed instead of 4.1.*

The maximum  $\sigma \in (0, 1)$  is unique:  $f(\sigma) = \max_{[0,1]} f(\rho) = f_M$ .

We define a **numerical grid** in  $\mathbb{R}^N \times (0, T)$  using the following notations:

- $\Delta x$  is the space grid size;
- $\Delta t$  is the time grid size;
- $(x_m, t_n) = (m\Delta x, n\Delta t)$  for  $n \in \mathbb{N}$  and  $m \in \mathbb{Z}$  are the grid points.

For a function  $v$  defined on the grid we write  $v_m^n = v(x_m, t_n)$  for  $m, n$  varying on a subset of  $\mathbb{Z}$  and  $\mathbb{N}$  respectively. We also use the notation  $u_m^n$  for  $u(x_m, t_n)$  when  $u$  is a continuous function on the  $(x, t)$  plane.

### 4.1 Godunov scheme [10, 11]

Consider the hyperbolic equation

$$u_t + F(u)_x = 0 \quad x \in \mathbb{R}, \quad t \in [0, T],$$

with initial data

$$u(x, 0) = u_0(x).$$

A solution of the problem is constructed taking a piecewise constant approximation of the initial data,  $v_0^\Delta$ . We set

$$v_m^0 = \frac{1}{\Delta x} \int_{x_m}^{x_{m+1}} u_0(x) dx, \quad m \geq 0 \quad (4.2)$$

and the scheme defines  $v_m^n$  recursively starting from  $v_m^0$ .

**Remark 4.2** *A wave starting from  $x_{m-1/2}$  will not reach the lines  $x = x_{m-1}$  and  $x = x_m$  before time  $t_{n+1}$  if*

$$\Delta t \sup_{m,n} \left\{ \sup_{u \in I(u_m^n, u_{m+1}^n)} |F'(u)| \right\} \leq \frac{1}{2} \Delta x. \quad (4.3)$$

Then we define the projection of the exact solution on a piecewise constant function

$$v_m^{n+1} = \frac{1}{\Delta x} \int_{x_m}^{x_{m+1}} v^\Delta(x, t_{n+1}) dx. \quad (4.4)$$

Since  $v$  is an exact solution of (2.1), we use the Gauss-Green formula in (2.1) to compute this value. Under the CFL condition

$$\Delta t \sup_{m,n} \left\{ \sup_{u \in I(u_m^n, u_{m+1}^n)} |F'(u)| \right\} \leq \Delta x \quad (4.5)$$

the waves do not influence the solutions in  $x = x_m$ , for  $t \in (t_n, t_{n+1})$ . Hence the solutions are locally given by the Riemann problems and in particular the flux in  $x = x_m$  for  $t \in (t_n, t_{n+1})$  is given by  $F(u(x_m, t)) = F(W_R(0; v_{m-1}^n, v_m^n))$ , where  $W_R(\frac{x}{t}; v_-, v_+)$  is the self-similar solution between  $v_-$  and  $v_+$ . As the flux is time invariant and continuous, we can put it out of the integral and, setting  $g^G(u, v) = F(W_R(0; u, v))$  under the condition (4.5), the scheme can be written as:

$$v_m^{n+1} = v_m^n - \frac{\Delta t}{\Delta x} (g^G(v_m^n, v_{m+1}^n) - g^G(v_{m-1}^n, v_m^n)). \quad (4.6)$$

The numerical flux  $g^G$ , for the flux we are considering, has the expression:

$$g^G(u, v) = \begin{cases} \min(f(u), f(v)) & \text{if } u \leq v, \\ f(u) & \text{if } v < u < \sigma, \\ f_M & \text{if } v < \sigma < u, \\ f(v) & \text{if } \sigma < v < u. \end{cases}$$

## 4.2 Kinetic method for a boundary value problem [3, 1]

Here we present the kinetic scheme for initial-boundary value conservation equations:

$$u_t + F(u)_x = 0, \quad (4.7)$$

$$u(x, 0) = u_0(x), \quad x \geq 0, \quad (4.8)$$

$$u(0, t) = u_b(t), \quad t \geq 0, \quad (4.9)$$

and (4.9) can be imposed only where it is compatible with the trace of the solution to the problem and with the flux  $F$ . We have  $u(x, t) \in \mathbb{R}$  for  $x \geq 0$ ,  $t \geq 0$ , and  $F$  is a Lipschitz continuous function.

A kinetic approximation of the problem (4.7) is obtained solving the following BGK-like system of  $N$  non-linear equations:

$$\partial_t f_k^\varepsilon + \lambda_k \partial_x f_k^\varepsilon = \frac{1}{\varepsilon} (M_k(u^\varepsilon) - f_k^\varepsilon), \quad (4.10)$$

where the  $\lambda_k$  are fixed velocities (a set of real numbers not all zero),  $\epsilon$  is a positive parameter, and each  $f_k^\epsilon$  is a function of  $\mathbb{R}^+ \times [0, T]$  with values in  $\mathbb{R}$ . We impose the corresponding initial and boundary data:

$$f_k^\epsilon(x, 0) = M_k(u_0(x)), \quad x \in \mathbb{R}^+, \quad (4.11)$$

$$f_k^\epsilon(0, t) = M_k(u_b(t)) \quad \forall \lambda_k > 0 \text{ and } t \geq 0. \quad (4.12)$$

Functions  $M_k$ ,  $k = 1, \dots, N$ , are the Maxwellian functions depending on  $u^\epsilon$ ,  $F$  and  $\lambda_k$ . To have the convergence of  $u^\epsilon = \sum_{k=1}^N f_k^\epsilon$  when  $\epsilon \rightarrow 0$  towards the solution of the problem (4.7), we need to impose the following compatibility conditions:

$$\sum_{k=1}^N M_k(u) = u, \quad \sum_{k=1}^N \lambda_k M_k(u) = F(u), \quad (4.13)$$

that show the link between problem (4.7) and system (4.10).

A sufficient condition for convergence is that  $M$  is Monotone Non Decreasing on  $I$ , [17]. Then the following subcharacteristic condition is satisfied for all  $u \in I$ :

$$\min_k \lambda_k \leq F'(u) \leq \max_k \lambda_k. \quad (4.14)$$

#### 4.2.1 Kinetic approximations.

Here follows a presentation of the different approximations we used in kinetic schemes already proposed in [17].

- **Two velocities model.**  $N = 2$ ,  $\lambda_1 = -\lambda_2 = -\lambda$ . We approximate the scalar conservation law (2.1) by a relaxation system which is diagonalized in the form

$$\begin{cases} \partial_t f_1^\epsilon - \lambda \partial_x f_1^\epsilon = \frac{1}{\epsilon} (M_1(u^\epsilon) - f_1^\epsilon) \\ \partial_t f_2^\epsilon + \lambda \partial_x f_2^\epsilon = \frac{1}{\epsilon} (M_2(u^\epsilon) - f_2^\epsilon). \end{cases}$$

The associated Maxwellian functions are

$$M_1(u) = \frac{1}{2} \left( u - \frac{F(u)}{\lambda} \right), \quad M_2(u) = \frac{1}{2} \left( u + \frac{F(u)}{\lambda} \right).$$

In order to respect the monotonicity condition MND on  $I \subset \mathbb{R}$ , we have the following relation for the velocity vector  $\lambda$ :

$$\max_{u \in I} |F'(u)| < \lambda. \quad (4.15)$$

- **Three velocities model.** Dealing with more velocities corresponds to more accurate approximation schemes. Take  $N = 3$  and the velocities  $\lambda_3 = -\lambda_1 = \lambda > 0$ ,  $\lambda_2 = 0$ . The approximated kinetic system has the Maxwellian functions given by

$$M_1(u) = \frac{1}{\lambda} \begin{cases} 0, & \text{if } u \leq \frac{1}{2}, \\ u(u-1) + \frac{1}{4}, & \text{if } u \geq \frac{1}{2}, \end{cases}$$



$$M_2(u) = \begin{cases} \left(1 - \frac{1}{\lambda}\right)u + \frac{1}{\lambda}u^2, & \text{if } u \leq \frac{1}{2}, \\ \left(1 + \frac{1}{\lambda}\right)u - \frac{1}{\lambda}u^2 - \frac{1}{2\lambda}, & \text{if } u \geq \frac{1}{2}, \end{cases}$$

$$M_3(u) = \frac{1}{\lambda} \begin{cases} u(1-u), & \text{if } u \leq \frac{1}{2}, \\ \frac{1}{4}, & \text{if } u \geq \frac{1}{2}. \end{cases}$$

At the boundary we impose  $f_3(0, t) = M_3(u_b(t))$  and the Maxwellian are MND if and only if the condition (4.15) is satisfied. In this case (4.15) reads

$$0 \leq M_2'(u) \leq 1 - \frac{|F'(u)|}{\lambda}.$$

This model, at first order, is the kinetic expression of the Engquist-Osher scheme.

#### 4.2.2 Numerical scheme

Following [3, 1], we discretize the problem (4.10)-(4.11)-(4.12) and making  $\epsilon$  tend to zero, we obtain a numerical scheme for the initial boundary value problem for the conservation law (4.7), see [1] for more details and convergence results. As usual, we discretize data of the problem by a piecewise constant approximation and we take for  $k = 1, 2, 3$ :

$$\begin{aligned} f_{-1,k}^n &= M_k(u_b^n), & 0 \leq n \leq M-1, \\ f_{m,k}^0 &= M_k(u_m^0), & m \in \mathbb{N}. \end{aligned}$$

The operators used to solve system (4.10) are splitted into the *transport* part and the *collision* part.

For the transport contribute, the scheme written in the Harten formulation including both first and second order in space approximation reads:

$$m \geq 0, \begin{cases} f_{m,k}^{n+\frac{1}{2}} = f_{m,k}^n(1 - D_{m-\frac{1}{2},k}^n) + D_{m-\frac{1}{2},k}^n f_{m-1,k}^n, & \text{if } \lambda_k > 0, \\ f_{m,k}^{n+\frac{1}{2}} = f_{m,k}^n(1 - D_{m+\frac{1}{2},k}^n) + D_{m+\frac{1}{2},k}^n f_{m+1,k}^n, & \text{if } \lambda_k \leq 0. \end{cases} \quad (4.16)$$

Note that it is necessary to assign the boundary value  $f_{b,k}^n = f_{-1,k}^n$  only for positive velocities. A first order in space upwind approximation is chosen:

$$D_{m-\frac{1}{2},k}^n = D_{m+\frac{1}{2},k}^n = \xi_k = |\lambda_k| \frac{\Delta t}{\Delta x}$$

and in that case (4.16) is well defined even for  $m = 0$ .

The transport part can be approximated by a second order scheme as follows. Starting from  $f_{m,k}^n$  we build a piecewise linear function:

$$\bar{f}_{m,k}^n(x) = f_{m,k}^n + (x - x_m)\sigma_{m,k}^n, \quad x \in (x_{m-\frac{1}{2}}, x_{m+\frac{1}{2}}),$$

where  $\sigma_{m,k}^n$  are limited slopes and we solve exactly the transport equations on  $[t_n, t_{n+1}]$ . Projecting the solution on the set of piecewise constant functions on

the cells, we obtain the explicit expression for  $D_{m+\frac{1}{2},k}^n$ :

$$D_{m+\frac{1}{2},k}^n = \xi_k \left( 1 + \operatorname{sgn}(\lambda_k) \Delta x \frac{(1 - \xi_k) (\sigma_{m+1,k}^n - \sigma_{m,k}^n)}{2 \Delta f_{m+\frac{1}{2},k}^n} \right), \quad (4.17)$$

with the convention that if  $\Delta f_{m+\frac{1}{2},k}^n = 0$ , then  $D_{m+\frac{1}{2},k}^n = \xi_k = |\lambda_k| \frac{\Delta t}{\Delta x}$ . Note that if  $\lambda_k > 0$  (4.17) is defined for  $m \geq -1$ , in the other cases is available for  $m \geq 0$ . The slopes  $\sigma_{m,k}^n$  for  $m \geq 1$  are:

$$\sigma_{m,k}^n = \operatorname{minmod} \left( \frac{\Delta f_{m+\frac{1}{2},k}^n}{\Delta x}, \frac{\Delta f_{m-\frac{1}{2},k}^n}{\Delta x} \right),$$

with  $\Delta f_{m+\frac{1}{2},k}^n = f_{m+1,k}^n - f_{m,k}^n$  and  $\operatorname{minmod}(a, b) = \min(|a|, |b|) \frac{\operatorname{sgn}(a) + \operatorname{sgn}(b)}{2}$ . For the convergence results see [1]. The time step restriction for both cases is

$$\max_{1 \leq k \leq N} |\lambda_k| \Delta t \leq \Delta x. \quad (4.18)$$

Then we use the solution obtained from the precedent scheme as the initial condition for collision system. Under the compatibility conditions (4.13) we find the exact solution of the system, that for  $\epsilon \rightarrow 0$  is

$$f_{m,k}^{n+1} = M_k(u_m^{n+\frac{1}{2}}) = M_k(u_m^{n+1}), \quad m \geq 0, \quad n \geq 1 \quad (4.19)$$

and the identity holds

$$u_m^{n+1} = \sum_k f_{m,k}^{n+\frac{1}{2}} = u_m^{n+\frac{1}{2}}. \quad (4.20)$$

Assuming that the Maxwellian functions are MND, we have the usual CFL condition

$$\max_u |F'(u)| \Delta t \leq \Delta x$$

and, from the transport part of the scheme, we have to impose the time step restriction in (4.18).

### 4.3 Boundary conditions and conditions at junctions

#### 4.3.1 Godunov scheme

**Boundary conditions.** Suppose to assign a condition at the incoming boundary  $x = 0$ :

$$u(0, t) = \rho_1(t) \quad t > 0$$

and study equation only for  $x > 0$ . Now we are considering the initial-boundary value problem (4.7)-(4.8)-(4.9) with  $u_0 \in C^1(\mathbb{R}^+)$ ,  $u_1(t) \in C^1((0, T))$ ,  $F \in C^1(\mathbb{R})$ . It is not easy to find a function  $u$  that satisfies (4.9) in a classical

sense, because, in general, the boundary data cannot be assumed. One seeks a condition which is to be effective only in the inflow part of the boundary. Following [4] the rigorous way of assigning the boundary condition is:

$$\max_{k \in I(u(0,t), \rho_1(t))} \left\{ \text{sgn}(u(0,t) - \rho_1(t)) [F(u(0,t)) - F(k)] \right\} = 0. \quad (4.21)$$

We practically proceed by inserting a ghost cell and defining

$$v_0^{n+1} = v_0^n - \frac{\Delta t}{\Delta x} (g^G(v_0^n, v_1^n) - g^G(u_1^n, v_0^n)), \quad (4.22)$$

where

$$u_1^n(t) = \frac{1}{\Delta t} \int_{t_n}^{t_{n+1}} \rho_1(t) dt$$

takes the place of  $v_{-1}^n$ .

An outgoing boundary can be treated analogously. Let  $x < L = x_N$ . Then the discretization reads:

$$v_N^{n+1} = v_N^n - \frac{\Delta t}{\Delta x} (g^G(v_N^n, u_2^n) - g^G(v_{N-1}^n, v_N^n)), \quad (4.23)$$

where

$$u_2^n(t) = \frac{1}{\Delta t} \int_{t_n}^{t_{n+1}} \rho_2(t) dt$$

takes the place of  $v_{N+1}^n$ , that is a ghost cell value.

**Conditions at a junction.** For roads connected to a junction at the right endpoint we set

$$v_N^{n+1} = v_N^n - \frac{\Delta t}{\Delta x} (\hat{\gamma}_i - g^G(v_{N-1}^n, v_N^n)),$$

while for roads connected to a junction at the right endpoint we have

$$v_0^{n+1} = v_0^n - \frac{\Delta t}{\Delta x} (g^G(v_0^n, v_1^n) - \hat{\gamma}_j),$$

where  $\hat{\gamma}_i, \hat{\gamma}_j$  are the maximized fluxes described in Section 2.

**Remark 4.3** For Godunov scheme there is no need to invert the flux  $f$  to put it in the scheme, as the Godunov flux coincides with the Riemann flux. In this case it suffices to insert the computed maximized fluxes directly in the scheme.

### 4.3.2 Kinetic schemes

**Boundary conditions.** For  $m = 0$  we take for the boundary

$$\sigma_{-1,k}^n = 0.$$

In this case, the slope  $\sigma_{0,k}^n$  can be defined as

- for  $\lambda_k > 0$ :

$$\sigma_{0,k}^n = \min\left(\frac{f_{1,k}^n - f_{0,k}^n}{\Delta x}, 2\frac{f_{0,k}^n - M_k(u_b^n)}{\Delta x}\right),$$

where  $u_b^n$  is the boundary condition;

- for  $\lambda_k < 0$ :

$$\sigma_{0,k}^n = \frac{f_{1,k}^n - f_{0,k}^n}{\Delta x}.$$

When  $m = N$  the scheme for  $\lambda_k < 0$  requires the values  $f_{N+1,k}^n, f_{N+2,k}^n$ , that can be obtained, for instance, by imposing a Neumann condition.

**Conditions at a junction.** As usual, in order to impose the boundary condition at a junction we need to examine the links between the roads. At the right boundary ( $m = N$ ) of roads linked to the junction on the right endpoint one has:

$$f_{N,k}^{n+\frac{1}{2}} = f_{N,k}^n(1 - D_{N+\frac{1}{2},k}^n) + D_{N+\frac{1}{2},k}^n f_{N+1,k}^n, \quad \text{for } \lambda_k < 0,$$

with

$$f_{N+1,k}^n = M_k(f^{-1}(\hat{\gamma}_i)).$$

Moreover we use the Neumann condition  $f_{N+2,k}^n = f_{N+1,k}^n$  for roads which are not linked to the junction on the right.

At the left boundary ( $m = 0$ ) of roads linked to the junction on the left endpoint the scheme in case  $\lambda_k > 0$  reads:

$$f_{0,k}^{n+\frac{1}{2}} = f_{0,k}^n(1 - D_{-\frac{1}{2},k}^n) + D_{-\frac{1}{2},k}^n f_{-1,k}^n,$$

with

$$f_{-1,k}^n = M_k(f^{-1}(\hat{\gamma}_j)).$$

Notice that  $\hat{\gamma}_i, \hat{\gamma}_j$  are the maximized incoming and outgoing fluxes obtained with the procedure described in Section 2, where the inversion of the flux function  $f$  follows the rules

- for roads entering the junction:
  - if  $u_N^n \in [0, \sigma]$  and  $\hat{\gamma}_i < F(u_N^n)$  then  $F^{-1}(\hat{\gamma}_i) \in [\tau(u_N^n), 1)$ ,
  - if  $u_N^n \in [0, \sigma]$  and  $\hat{\gamma}_i = F(u_N^n)$  then  $F^{-1}(\hat{\gamma}_i) = u_N^n$ ,
  - if  $u_N^n \in [\sigma, 1]$  then  $F^{-1}(\hat{\gamma}_i) \in [\sigma, 1]$ ,

with  $i = 1, 2$ ;

- for roads coming out of the junction:
  - if  $u_0^n \in [\sigma, 1]$  and  $\hat{\gamma}_j < F(u_0^n)$  then  $F^{-1}(\hat{\gamma}_j) \in [0, \tau(u_0^n))$ ,
  - if  $u_0^n \in [\sigma, 1]$  and  $\hat{\gamma}_j = F(u_0^n)$  then  $F^{-1}(\hat{\gamma}_j) = u_0^n$ ,
  - if  $u_0^n \in [0, \sigma]$  then  $F^{-1}(\hat{\gamma}_j) \in [0, \sigma]$ ,

with  $j = 1, 2$ .

Recall that  $u_m^n$  indicates a macroscopic variable and it represents a density.

## 5 Tests

In this Section we present some numerical tests performed with the schemes previously introduced, such as the Godunov scheme (G), the three-velocities Kinetic scheme of first order ( $3VK_1$ ) and the three-velocities Kinetic method ( $3VK_2$ ) with  $\lambda_3 = -\lambda_1 = 1.0$  and  $\lambda_2 = 0$ . In general the three-velocities models work better than the two-velocities ones. We introduce the formal numerical order  $\gamma$  of a numerical method as an average in the following way:

$$\gamma = \frac{1}{R} \sum_{r=1}^R \gamma_r, \quad (5.1)$$

where

$$\gamma_r = \log_2 \left( \frac{e^r(1)}{e^r(2)} \right), \quad r = 1, \dots, R, \quad (5.2)$$

with  $r$  the index of roads composing the network. The  $L^1$ -error on each road is

$$e^r(p) = \frac{h}{p} \sum_{j=0, \dots, pN} \left| w_j^{pM} \left( \frac{h}{p} \right) - w_{2j}^{pM} \left( \frac{h}{2p} \right) \right| \quad p = 1, 2, r = 1, \dots, R, \quad (5.3)$$

where  $w_m^M(h)$  denotes the numerical solution obtained with the space step discretization equal to  $h$ , computed in  $x_m$  at the final time  $t_M = T$ ,  $R$  indicates the number of roads in the network. The total  $L^1$ -error is

$$TOT_{err} = \sum_{r=1}^R e^r(1). \quad (5.4)$$

### 5.1 Bottleneck

Now we want to present some numerical approximations to the equation (2.1) with fluxes (3.1) and (3.2). The next tables provide a comparison between the three methods in terms of  $L^1$ -error and order of convergence  $\gamma$ .

Here we deal with a road of length 2 parametrized by the interval  $[0, 2]$  with the separation point placed in the middle of the road, namely  $x = 1$ . The numerical schemes used to provide the approximated solution are Godunov scheme (G), three-velocities Kinetic scheme of first order ( $3VK_1$ ) and second order ( $3VK_2$ ) with the following velocities:  $\lambda_3 = -\lambda_1 = 1.0$  and  $\lambda_2 = 0$ .

**Test B1.** Let us take the following initial and boundary data

$$\rho_1(0, x) = 0.66, \quad \rho_2(0, x) = 0.66, \quad \rho_{1,b}(t, 0) = 0.25. \quad (5.5)$$

Since the initial value 0.66 is very close to the maximum value that can be absorbed by road 2, after a short time, namely  $T = 2$ , the formation of a traffic jam can be observed, see Figures 9.

$h$	G		$3VK_1$		$3VK_2$	
	$\gamma$	$L^1$ Error	$\gamma$	$L^1$ Error	$\gamma$	$L^1$ Error
0.1	1.51554	3.347e-002	1.14981	2.886e-002	1.19519	2.931e-002
0.05	0.89752	1.170e-002	0.83645	1.301e-002	0.92098	1.280e-002
0.025	0.58367	6.285e-003	0.85088	7.284e-003	0.75549	6.761e-003
0.0125	1.22648	4.194e-003	1.16427	4.038e-003	1.29260	4.005e-003
0.00625	0.65763	1.792e-003	0.83753	1.802e-003	0.73386	1.635e-003
0.003125	1.50268	1.136e-003	1.12176	1.008e-003	1.50429	9.830e-004

TABLE B1-1: Orders and errors of the approximation schemes Godunov (G), Kinetic of first order ( $3VK_1$ ) and of second order ( $3VK_2$ ) for data (5.5),  $T = 0.5$ .

$h$	G	$3VK_1$	$3VK_2$
	$L^1$ Error	$L^1$ Error	$L^1$ Error
0.1	2.07651e-002	2.19038e-002	2.41712e-002
0.05	1.25376e-002	1.45365e-002	1.35243e-002
0.025	8.38778e-003	8.07708e-003	8.00970e-003
0.0125	3.58458e-003	3.60392e-003	3.26967e-003
0.00625	2.27234e-003	2.01675e-003	1.96603e-003
0.003125	8.01899e-004	9.26764e-004	8.49835e-004

TABLE B1-2: Errors of the approximation schemes Godunov (G), Kinetic of first order ( $3VK_1$ ) and of second order ( $3VK_2$ ) for data (5.5),  $T = 1.0$ .

**Test B2.** Let us assume the road is initially empty and take the following initial and boundary data

$$\rho_1(0, x) = \rho_2(0, x) = 0, \quad \rho_{1,b}(t, 0) = 0.4. \quad (5.6)$$

Since  $\rho_{1,b} > \bar{\rho} \simeq 0.21$ , even in this case there is a jam formation as showed by Figures 10. Tables of orders and errors follow.

$h$	G		$3VK_1$		$3VK_2$	
	$\gamma$	$L^1$ Error	$\gamma$	$L^1$ Error	$\gamma$	$L^1$ Error
0.1	0.65705	1.841e-002	0.65705	1.841e-002	0.81414	1.2733e-002
0.05	0.67659	1.167e-002	0.67659	1.168e-002	0.82570	7.2418e-003
0.025	0.70677	7.305e-003	0.70676	7.306e-003	0.84143	4.0859e-003
0.0125	0.73821	4.476e-003	0.73821	4.476e-003	0.85393	2.2803e-003
0.00625	0.76816	2.683e-003	0.76816	2.683e-003	0.86470	1.2616e-004
0.003125	0.79447	1.575e-003	0.79447	1.575e-003	0.87441	6.9283e-004

TABLE B2-1: Orders and errors of the approximation schemes Godunov (G), Kinetic of first order ( $3VK_1$ ) and of second order ( $3VK_2$ ) for data (5.6),  $T = 1$ .

$h$	G	$3VK_1$	$3VK_2$
	$L^1$ Error	$L^1$ Error	$L^1$ Error
0.1	2.16316e-002	2.18455e-002	1.69308e-002
0.05	7.10040e-003	1.09717e-002	1.09403e-002
0.025	4.70270e-003	5.44031e-003	3.70921e-003
0.0125	2.48223e-003	2.61377e-003	2.61455e-003
0.00625	1.09907e-003	8.57023e-004	7.89821e-004
0.003125	5.80967e-004	3.61744e-004	2.75442e-004

TABLE B2-2: Errors of the approximation schemes Godunov (G), Kinetic of first order ( $3VK_1$ ) and of second order ( $3VK_2$ ) for data (5.6),  $T = 4$ .

From the analysis of the previous Tables we can see that both  $3VK_1$  and  $3VK_2$  perform better than the Godunov scheme. In fact, the kinetic schemes show a good stability even after the interaction at the junction.

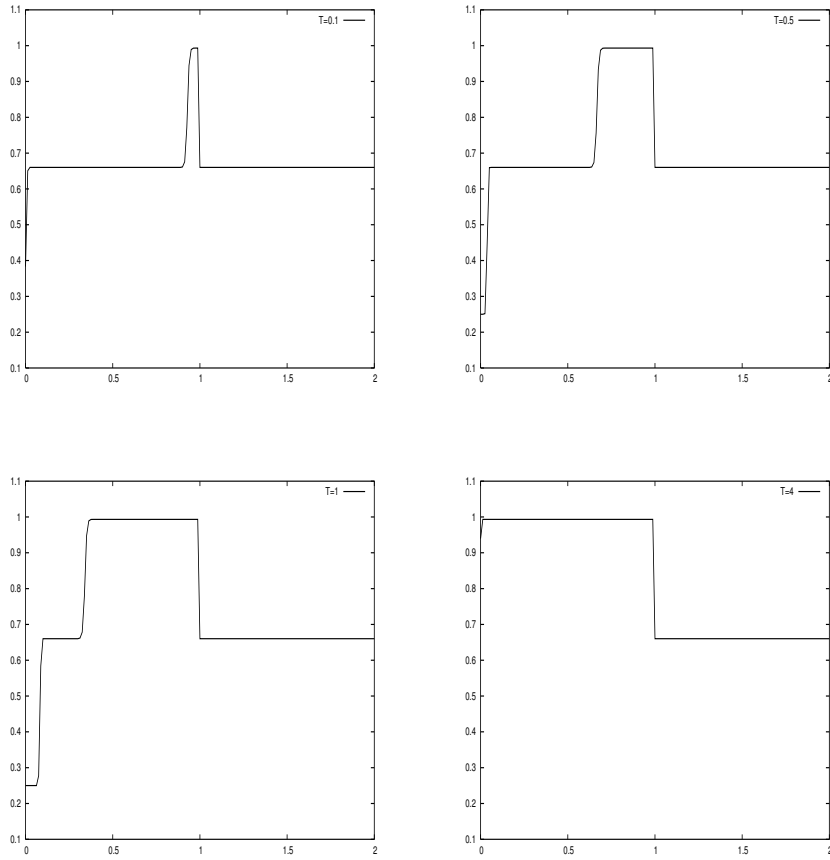


Figure 9: Evolution in time for data (5.5) computed by  $3VK_2$  scheme,  $h = 0.0125$ .



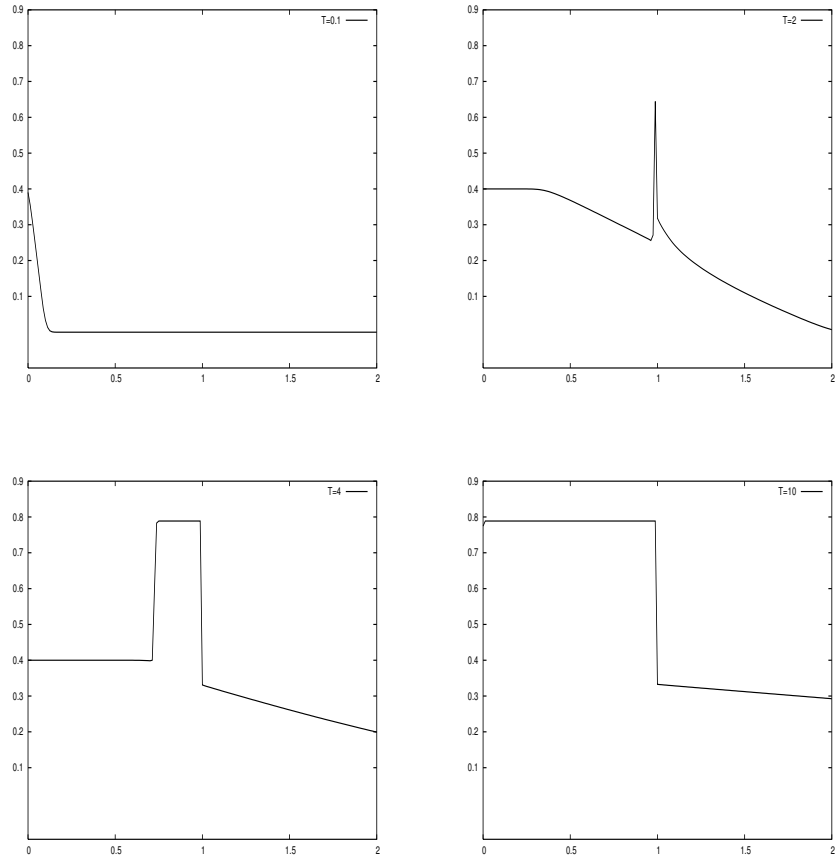


Figure 10: Evolution in time for data (5.6) computed by  $3VK_2$  scheme,  $h = 0.0125$ .

## 5.2 Two incoming - two outgoing roads

Recall definitions of Section 3 of junction  $J$  with two incoming roads and two outgoing roads all parametrized with the interval  $[0, 1]$ . Here we refer to the situation described in Appendix of [8], where the coefficients of the distribution matrix  $A$  are such that  $0 < \alpha_{32} < \alpha_{31} < 1/2$ . We set

$$\alpha_{31} = \alpha_1, \quad \alpha_{32} = \alpha_2, \quad \alpha_{41} = 1 - \alpha_1, \quad \alpha_{42} = 1 - \alpha_2$$

and we introduce the notation

$$\rho_1(0, x) = \rho_{1,0}, \quad \rho_2(0, x) = \rho_{2,0}, \quad \rho_3(0, x) = \rho_{3,0}, \quad \rho_4(0, x) = \rho_{4,0}.$$

The distribution matrix is fixed as

$$A = \begin{pmatrix} 0.4 & 0.3 \\ 0.6 & 0.7 \end{pmatrix} \quad (5.7)$$

and we consider the following constant initial and boundary data

$$\begin{aligned} \rho_{1,0} = \rho_{4,0} = \sigma, \quad \rho_{2,0} = \rho_{3,0} = f^{-1}\left(\frac{\alpha_1}{1 - \alpha_2} f(\sigma)\right) &= 0.82732683535, \\ \rho_{1,b}(0, t) = \sigma, \quad \rho_{2,b}(0, t) = f^{-1}\left(\frac{\alpha_1}{1 - \alpha_2} f(\sigma)\right) &= 0.82732683535. \end{aligned} \quad (5.8)$$

**Remark 5.1** *Notice that the boundary condition is imposed only on the incoming roads, as for the outgoing ones we use a Neumann condition at the final endpoint.*

Let us introduce a perturbation on the initial data of road 1

$$\rho_1(0, x) = \begin{cases} \rho_{1,0} = \sigma & \text{if } 0 \leq x \leq 0.5, \\ \rho_1 & \text{if } x \geq 0.5, \end{cases} \quad (5.9)$$

and  $\rho_1, \rho_{1,0}, \rho_{2,0}, \rho_{3,0}, \rho_{4,0}$  be constants such that

$$\sigma < \rho_{2,0} < 1, \quad \sigma < \rho_{3,0} < 1, \quad \rho_1 < \sigma, \quad \rho_{1,0} = \rho_{4,0} = \sigma, \quad (5.10)$$

$$f(\rho_{1,0}) = f(\rho_{4,0}) = f(\sigma), \quad f(\rho_{2,0}) = f(\rho_{3,0}) = \frac{\alpha_1}{1 - \alpha_2} f(\sigma),$$

so that  $(\rho_{1,0}, \rho_{2,0}, \rho_{3,0}, \rho_{4,0})$  is an equilibrium configuration.

In (5.9) assume to have a small perturbation represented by  $\rho_1 = 0.4$  and let the boundary data on road 1 be  $\rho_{1,b} = 0.4$ . The initial data on other roads of the junction, namely  $\rho_{2,0}, \rho_{3,0}, \rho_{4,0}$ , are taken as in (5.8) and the boundary data on road 2 is  $\rho_{1,b} = \rho_{2,0}$ . After a certain time ( $t \sim 8$ ) the wave  $(\rho_1, \rho_{1,0})$  interacts with the junction thus determining a shock wave travelling on road 3. At time  $T = 470$  a new equilibrium configuration is reached: the value of density on road 4 remains constant and on road 2 the final density is very close the initial

value  $\rho_{2,0}$ . In Figures 11, 12 and 13 we describe the evolution in time of road 1 and road 3, where numerical solutions were produced by the  $3VK_2$  scheme. The following tables T1 and T2 report orders and  $L^1$ -errors of the schemes, defined by (5.2), respectively before and after the interaction at the junction. Looking at Table T2 one can observe that the accuracy of kinetic methods is higher respect to Godunov scheme. This reveals that Godunov scheme is more diffusive. Notice that in this case for  $3VK_2$  scheme we used the boundary condition  $\sigma_{0,k}^n = 0$  for  $\lambda_k < 0$ .

$h$	G		$3VK_1$		$3VK_2$	
	$\gamma$	$L^1$ Error	$\gamma$	$L^1$ Error	$\gamma$	$L^1$ Error
0.2	1.4	6.01235e-003	1.4	6.00949e-003	1.9	6.72896e-003
0.1	0.88	2.27825e-003	0.88	2.27511e-003	0.94	1.82122e-003
0.05	0.93	1.23890e-003	0.93	1.23605e-003	0.98	9.49608e-004
0.025	0.97	6.51197e-004	0.98	6.48354e-004	0.99	4.81271e-004
0.0125	0.98	3.32129e-004	0.99	3.29293e-004	0.99	2.41161e-004
0.00625	0.98	1.67647e-004	1.0	1.65002e-004	1.0	1.20602e-004

TABLE T1 Convergence order  $\gamma$  and errors of the approximation schemes Godunov(G), kinetic 3-velocities of first order ( $3VK_1$ ) and second order ( $3VK_2$ ), for  $T = 1$ .

$h$	G	$3VK_1$	$3VK_2$
	$L^1$ Error	$L^1$ Error	$L^1$ Error
0.2	1.11248e-001	5.58553e-002	5.53875e-002
0.1	4.56467e-002	2.24683e-002	2.07874e-002
0.05	1.21337e-002	9.74289e-003	6.93735e-003
0.025	1.17982e-002	5.76965e-003	5.41827e-003
0.0125	1.16302e-002	8.02476e-003	8.04770e-003
0.00625	7.44115e-003	5.62481e-003	5.63628e-003

TABLE T2  $L^1$ -errors of the approximation schemes Godunov(G), kinetic 3-velocities of first order ( $3VK_1$ ) and second order ( $3VK_2$ ) obtained using the exact solution at time  $T = 20$ .

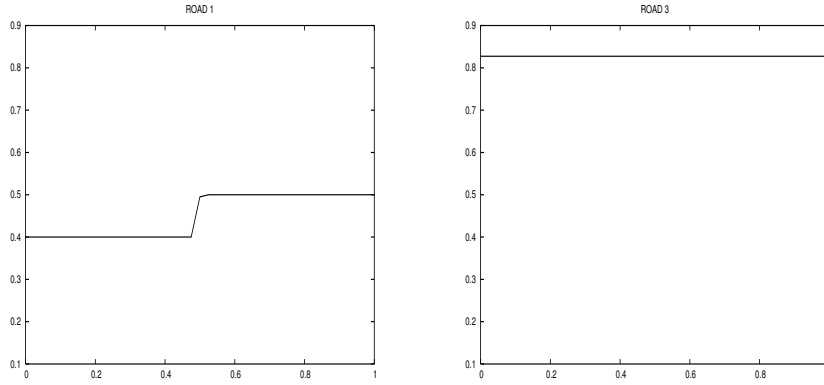


Figure 11: Initial configuration of data (5.9) with  $\rho_1 = 0.4 = \rho_{1,b}$  at time  $T = 0$ , with  $h = 0.025$ .

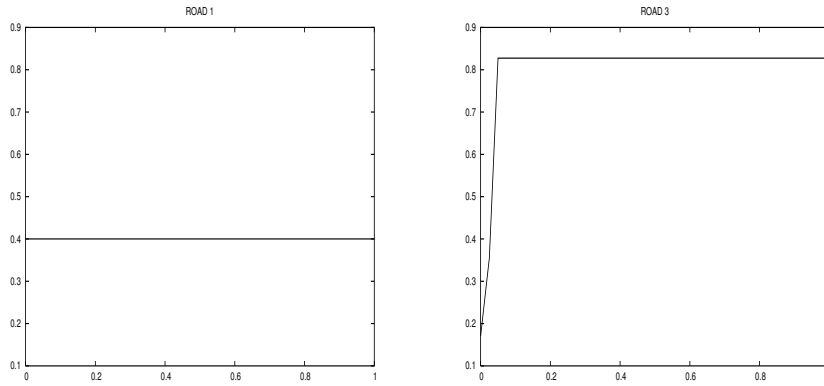


Figure 12: Situation after the interaction,  $T = 25$ ,  $h = 0.025$ .

### 5.3 Traffic circles

In the next pages we present some simulations reproducing a simple traffic circle composed by 8 roads and 4 junctions. The numerical solutions have been generated by the  $3VK_2$  method for  $h = 0.025$  and  $cfl = 0.5$ .

Consider the following initial and boundary data

$$\begin{aligned}
 \rho_1(0, x) &= 0.25, \quad \rho_2(0, x) = 0.4, \quad \rho_3(0, x) = 0.5, \quad \rho_4(0, x) = 0.5, \quad (5.11) \\
 \rho_{1R}(0, x) &= 0.5, \quad \rho_{2R}(0, x) = 0.5, \quad \rho_{3R}(0, x) = 0.5, \quad \rho_{4R}(0, x) = 0.5, \\
 \rho_{1,b}(t, 0) &= 0.25, \quad \rho_{2,b}(t, 0) = 0.4.
 \end{aligned}$$

The distribution coefficients, namely  $(\alpha_{1R,3}, \alpha_{1R,2R}, \alpha_{3R,4}, \alpha_{3R,4R})$ , are assumed

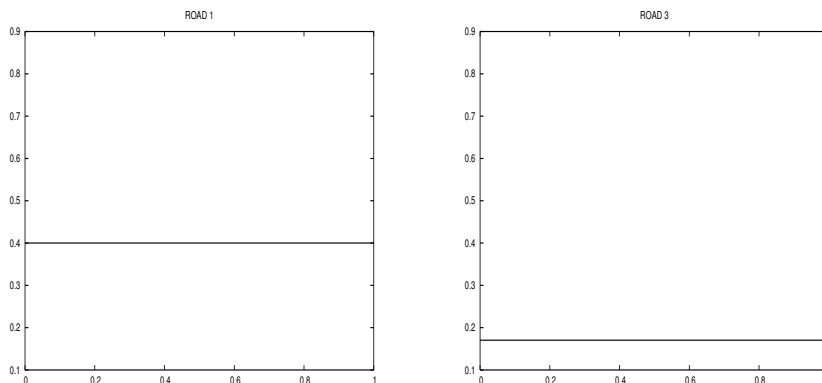


Figure 13: Final configuration,  $T = 470$ ,  $h = 0.025$ .

to be constant and are all equal to  $\alpha = 0.5$ . Let us choose the following priority parameters, which are  $q_1 = q(1, 4R, 1R) = 0.25$ ,  $q_2 = q(2, 2R, 3R) = 0.25$ . The fixed values imply that road  $4R$  is the through street respect to road 1 and road  $2R$  is the through street respect to 1. The evolution in time of traffic is reported in the next Figures 14. Observe that at time  $t = 5$  shocks are generated on the entering roads 1 and 2, while rarefaction waves in the direction of traffic are created on roads  $4R$ ,  $2R$ , 3, 4. Roads  $1R$  and  $3R$  do not change the level of the density. At  $t = 10$  rarefaction waves travelling in the sense of traffic produce a decrease in the car density on roads  $4R$ ,  $3R$ , 3, 4. On entering roads 1 and 2 the effect of shocks travelling backwards is a considerable increase of the density and, again, roads  $1R$  and  $3R$  have the same configuration, which corresponds to the maximum flux. At time  $T = 40$  the roads entering in the circle have an high value of density as they wait at the junctions, while densities of roads in the circle are lowered due to the fact that traffic is flowing towards the outgoing roads 3 and 4. We can observe that starting from the same configuration (5.11) but setting differently the right of way parameters, traffic within the circle is fluid and is distributed between the outgoing roads.

Fig. 15, obtained for data (5.11) and  $q_1 = q_2 = 0.5$ , shows a situation quite similar to that in Fig. 14. The difference is represented by the values of density on the roads  $2R$  and  $4R$  that reveal a shock formation with zero speed. As a consequence, the time for covering the path of the circle from road 1 to road 4 is higher than in the case depicted in Fig. 14. In particular, let  $\delta$  be the portion of road  $2R$  at the lowest value of density, i.e. 0.15, and  $1 - \delta$  the other portion of the same road, we can estimate the time for covering the path from road 1 to road 4. In the first case is

$$\frac{1}{0.5} + \frac{1}{0.85} + \frac{1}{0.5} \sim 5.17$$

while here (with  $\delta = 0.5$ ) we get

$$\frac{1}{0.5} + \frac{\delta}{0.85} + \frac{1-\delta}{0.15} + \frac{1}{0.5} \sim 7.92$$

and the difference between the previous and the current case is

$$\Delta t = \frac{1-\delta}{0.15} - \frac{1-\delta}{0.85} = (1-\delta)\frac{80}{17},$$

that is greater as  $\delta \rightarrow 0$ .

Let us set the right of way parameters as  $q_1 = q(1, 4R, 1R) = 0.75$ ,  $q_2 = q(2, 2R, 3R) = 0.75$ . This means that road 1 is the through street respect to road  $4R$  and road 2 is the through street respect to  $2R$ . As before, the distribution coefficients are assumed to be constant and all equal to  $\alpha = 0.5$ . The evolution in time of traffic densities is described in Figure 16. One can observe that at time  $t = 1.5$  the chosen right of way parameters provoke shocks propagating backwards along roads  $2R$  and  $4R$  and consequently a shock is created on road 2. Successively, the density on roads  $4R$ ,  $2R$  increases and shocks are propagating backwards on roads  $1R$  and  $3R$ . Roads 3 and 4 show a very low density of cars. At  $T = 40$  densities on the incoming roads and within the circle (all equal to the maximum value  $\rho_{\max} = 1$ ), represent a situation of traffic jam, the so called bumper-to-bumper traffic. This means that no cars can exit the circle, as showed by the fact that roads 3 and 4 are empty. Hence, in that case, the choice of the right of way parameter determines a situation of completely blocked traffic.

In the next pages, Figures 16, 14, 15 show the evolution in time of the density for the discussed cases with the following legend:

Legend	
$t = 0$	—
$t = 5$	—+—
$t = 10$	—×—
$t = 40$	—□—

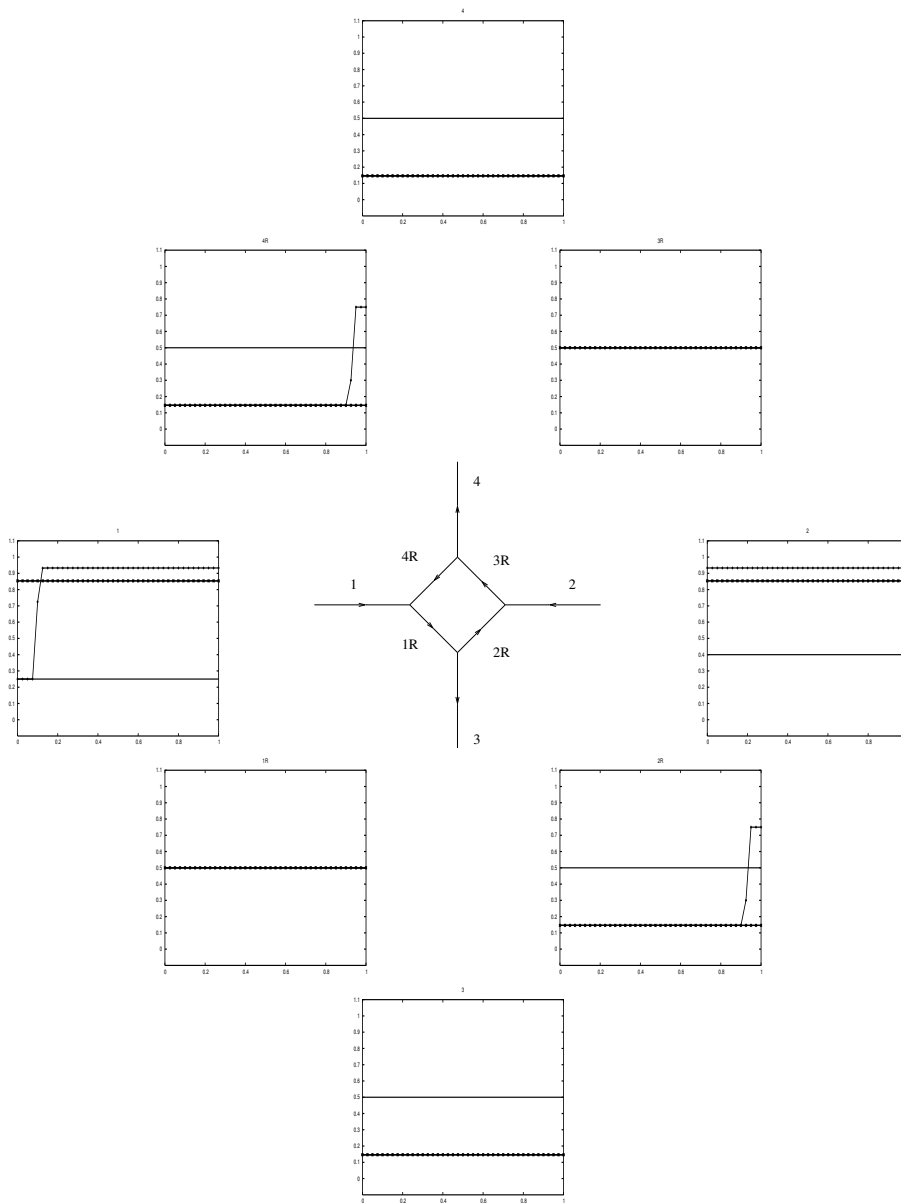


Figure 14: Traffic circle with  $q_1 = q_2 = 0.25$ .

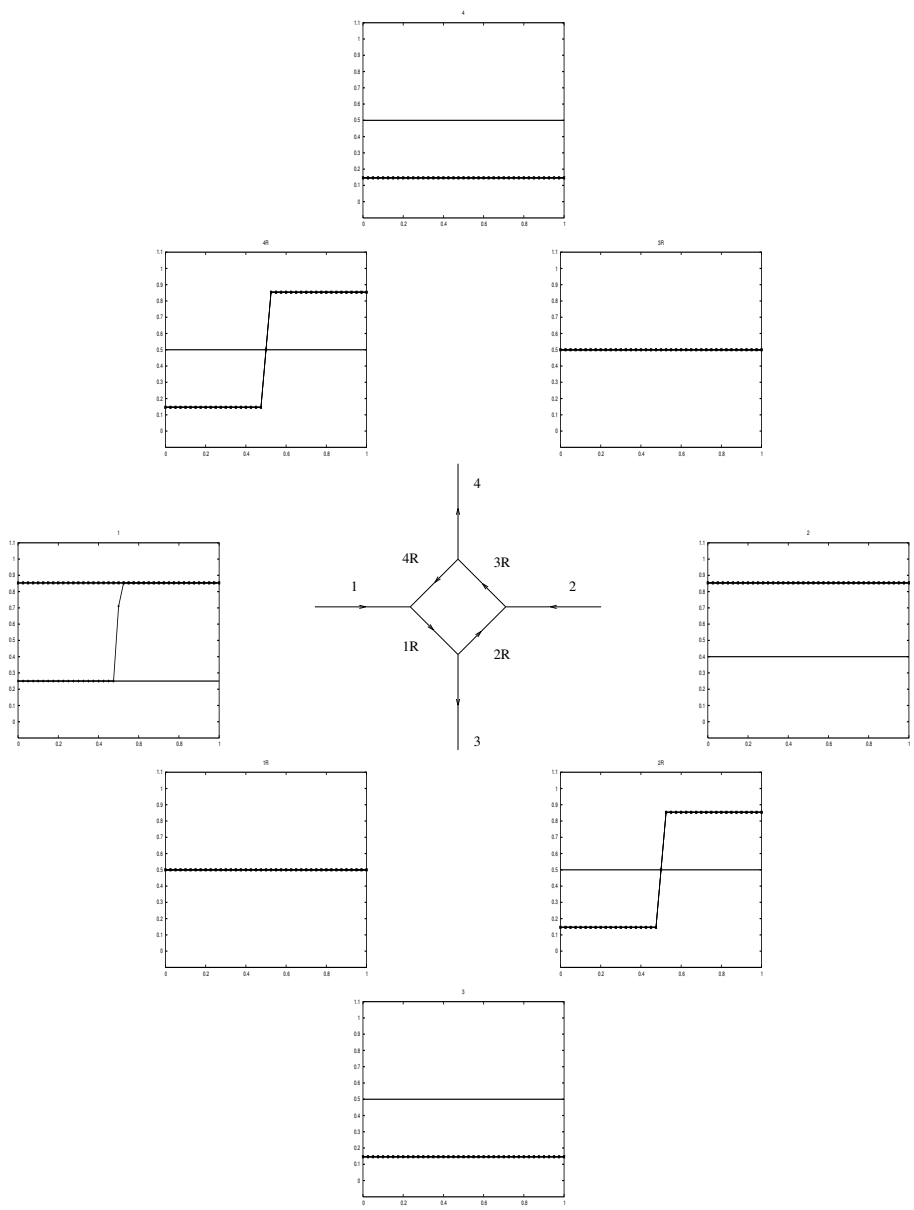


Figure 15: Traffic circle with  $q_1 = q_2 = 0.5$ .



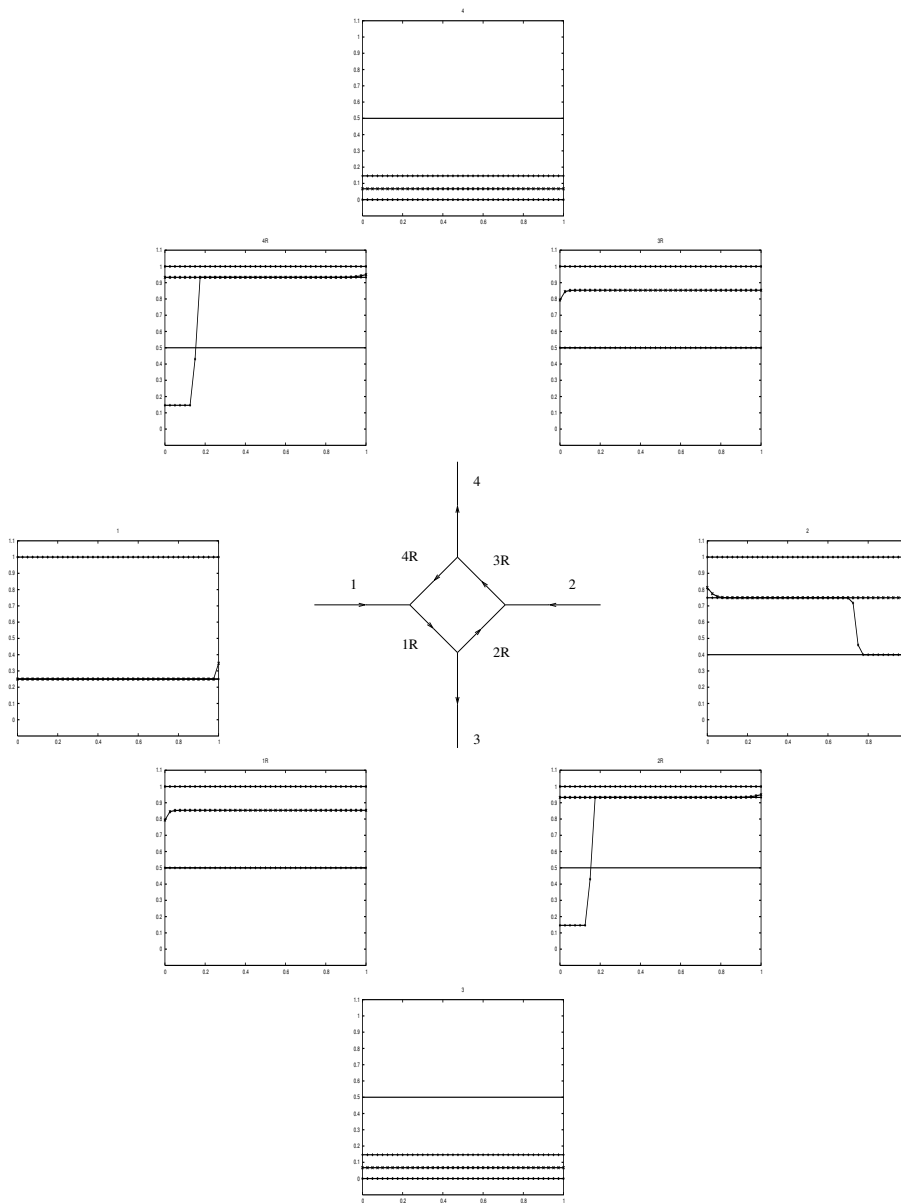


Figure 16: Traffic circle with  $q_1 = q_2 = 0.75$ .



## References

- [1] D. Aregba-Driollet, V. Milišić, Kinetic Approximation of a Boundary Value Problem for Conservation Laws, *Numerische Mathematik* **97** (2004), pp. 595-633.
- [2] V. Astarita, Node and Link Models for Network Traffic Flow Simulation, *Mathematical and Computer Modelling* **35** (2002), pp. 643-656.
- [3] D. Aregba-Driollet, R. Natalini, Discrete Kinetic Schemes for Multidimensional Systems of Conservation Laws, *SIAM J. Numer. Anal.* **37** (2000), No. 6, pp. 1973-2004.
- [4] C. Bardos, A. Y. Le Roux, J. C. Nédélec, First Order Quasilinear Equation with Boundary Conditions, *Commun. Partial Differential Equations*, **4** (1979), pp. 1017-1034.
- [5] A. Bressan, Hyperbolic systems of conservation laws. The one-dimensional Cauchy problem. Oxford Lecture Series in Mathematics and its Applications. 20. Oxford University Press (2000).
- [6] G. Bretti, A. Sgalambro,  
<http://www.iac.rm.cnr.it/~bretti/TrafficNumericalSolution.html> .
- [7] Y. Chitour, B. Piccoli, Traffic circles and timing of traffic lights for cars flow, *Discrete and Continuous Dynamical Systems-Series B* (to appear).
- [8] G. M. Coclite, M. Garavello, B. Piccoli, Traffic Flow on a Road Network, *Siam Math. Anal.* (to appear).
- [9] C.M. Dafermos, Hyperbolic conservation laws in continuum physics. Grundlehren der Mathematischen Wissenschaften. 325. Berlin: Springer (2000).
- [10] S.K. Godunov, A finite difference method for the numerical computation of discontinuous solutions of the equations of fluid dynamics, *Mat. Sb.* **47**, 1959, pp. 271-290.
- [11] E. Godlewski, P.A. Raviart, Hyperbolic systems of conservation laws, *Mathématiques & Applications [Mathematics and Applications]*, 3/4. Ellipses, Paris (1991).
- [12] R. Haberman, *Mathematical models*, Prentice-Hall, Inc. New Jersey, 1977, pp. 255-394.
- [13] H. Holden and N. H. Risebro, A Mathematical Model of Traffic Flow on a Network of Unidirectional Roads, *SIAM J. Math. Anal.*, **26** (1995), pp. 999-1017.
- [14] A. Klar, Kinetic and macroscopic traffic flow models, Lecture notes for the XX School of Computational Mathematics, "Computational aspects in kinetic models", Piano di Sorrento (Italy) September 22-28, 2002.
- [15] R.J. Leveque, *Finite volume methods for hyperbolic problems*. Cambridge Texts in Applied Mathematics. Cambridge University Press (2002).

- [16] M. J. Lighthill, G. B. Whitham, On kinematic waves. II. A theory of traffic flow on long crowded roads. *Proc. Roy. Soc. London. Ser. A.*, **229** (1955), pp. 317–345.
- [17] R. Natalini, A Discrete Kinetic Approximation of Entropy Solutions to Multidimensional Scalar Conservation Laws, *Journal of differential equations*, **148** (1998), pp. 292-317.
- [18] P. I. Richards, Shock Waves on the Highway, *Oper. Res.*, **4** (1956), pp. 42–51.
- [19] G.B. Whitham, Linear and nonlinear waves. Pure and Applied Mathematics. A Wiley-Interscience Series of Texts, Monographs, and Tracts. New York etc.: John Wiley & Sons. (1974).